CHEMISTRY
A European Journal

A Journal of
ChemPubSoc Europe

Accepted Article

Title: Ferrichrome has found its match: biomimetic analogs with diversified activity map discrete microbial targets

Authors: Jenny Besserglick, Evgenia Olshvang, Agnieszka Szebesczyk, Joseph Englander, Dana Levinson, Yitzhak Hadar, Elzbieta Gumienna-Kontecka, and Abraham Shanzer

To be cited as: *Chem. Eur. J.* 10.1002/chem.201702647

Link to VoR: http://dx.doi.org/10.1002/chem.201702647

Supported by
ACES

WILEY-VCH

10.1002/chem.201702647

WILEY-VCH

FULL PAPER

Ferrichrome has found its match: biomimetic analogs with diversified activity map discrete microbial targets

Jenny Besserglick,[a] Evgenia Olshvang,[a] Agnieszka Szebesczyk,[b] Joseph Englander,[a] Dana Levinson,[c] Yitzhak Hadar,[c] Elzbieta Gumienna-Kontecka*[b], and Abraham Shanzer*[a]

Abstract: Siderophores provide an established platform for studying molecular recognition principles in biological systems. Herein we describe the preparation of ferrichrome biomimetic analogs varying in length and polarity of the amino acid chain separating between the tripodal scaffold and the pendent Fe^{III} chelating hydroxamic acid groups. Spectroscopic and potentiometric titrations determined their iron affinity to be within the range of efficient chelators. Microbial growth promotion and iron uptake studies were conducted on *E. coli*, *P. putida* and *U. maydis*. A wide range of siderophore activity was observed in the current series: from a rare case of a species-specific growth promotor in *P. putida* to an analog matching ferrichrome in cross-phylum activity and uptake pathway. A fluorescent conjugate of the broad-range analog visualized siderophore destination in bacteria (periplasmic space) vs fungi (cytosol) mapping new therapeutic targets. Quantum Dots (QD) decorated with the most potent FC analog provided a tool for immobilization of ferrichrome-recognizing bacteria. Bacterial clusters formed around QDs may provide a platform for their selection and concentration.

Introduction

Siderophores are low molecular weight organic chelators, bio-synthesized and secreted by microorganisms to sequester environmental iron - a vital nutrient for a variety of essential cellular processes.[1] Often the iron-siderophore complex is recognized by specialized microbial outer-membrane receptors, which trigger its uptake by a cascade of transporting events.[2] Finally the iron is released in the cytosol and the siderophore is usually recycled to acquire additional iron.[3] While the iron uptake mechanism has been extensively studied[1b, 4] their recycling processes mostly remain elusive.[5]

Siderophores usually encapsulate the ferric ion by a variety of hard donor bidentate ligands,[6] most common being catechols, hydroxamates[7] and α-hydroxy carboxylic acids.[4a]

[a] Dr. J. Besserglick, Dr. E. Olshvang, Dr. J. Englander, Prof. Dr. A. Shanzer; Department of Organic Chemistry,
The Weizmann Institute of Science, Rehovot 7610001, Israel.
E-mail: abraham.shanzer@weizmann.ac.il
[b] Dr. A. Szebesczyk, Dr. E. Gumienna-Kontecka; Faculty of Chemistry, University of Wrocław, F. Joliot-Curie 14, 50-383 Wrocław, Poland.
E-mail: elzbieta.gumienna-kontecka@chem.uni.wroc.pl
[c] D. Levinson ,Prof. Dr. Y. Hadar;
Department of Plant Pathology and Microbiology, The R.H. Smith Faculty of Agriculture Food and Environment
The Hebrew University of Jerusalem, Rehovot 7610001, Israel.

Supporting information for this article is given via a link at the end of the document.

Ferrichrome[8] (FC) is an archetype of a natural hydroxamate siderophore. Although of fungal origin, it can be recognized by numerous bacterial species.[9] It is composed of a cyclic hexapeptide ring template, non-symmetrically extended by three identical L-ornithine derived arms each terminated by a hydroxamate moiety. Together, the three bidentate hydroxamates delineate an octahedral cavity matching the geometrical requirement of the ferric ion.

Although over the years some elegant synthetic routes to native siderophores were demonstrated,[10] they are still often complex and tedious to synthesize.[11] Let alone to obtain their conjugates,[12] due to lack of residual moieties for functionalization with fluorescent markers, surface active molecules or drugs. In this respect, FC is no different from other siderophores.

An alternative approach attempts to reproduce the function rather than the detailed structure of a biological substrate. Once a biologically active scaffold is found, it can be further diversified and tuned. This method, known as biomimetic chemistry,[13] has been applied for preparation of artificial siderophores,[9, 14] and in our group we have focused on synthetic FC analogs.[15] Their structure relies on four basic elements: (i) the C3 symmetric tris–carboxylate template, replacing the native FC hexapeptide; (ii) template extension with natural amino acid derived arms; (iii) retrohydroxamate ligand, with order reversed with respect to the native hydroxamate moiety;[16] (iv) apical site for efficient conjugation, that interferes neither with iron binding, nor with receptor recognition.

This approach resulted in efficient preparation of multiple FC analogs with biological activity and their enantio-pure iron complexes for exploring transporters' stereo-specific preferences.[17] [18] Moreover, analogs conjugated with surface adhesive functionalities, drug candidates and fluorescent tags[19] for visualizing their 'trafficking' and compartmentalization have been prepared. Owing to their modularity, tripodal FC analogs were successfully utilized beyond siderophore biology, for example as molecular switches[20] and sensors.[21]

So far, this methodology did not overcome some inherent limitations including: (i) low overall number of FC analogs capable of promoting microbial growth, particularly in *E. coli* and (ii) the fact that activity across multiple species, similar to native FC, was obtained only sporadically.

To overcome these limitations, we resorted to the detailed structure of FC in its transporter of *E. coli* - Ferric Hydroxamate Uptake protein component A (FhuA). FhuA is still among the few siderophore transporters with a resolved crystal structure.[22] The model derived from X-ray diffraction analysis designates tight contacts between the protein transporter and the iron binding moiety of FC (please refer to Supporting information, Figure S1). We assumed that these contacts might have been disrupted by bulky groups in the immediate vicinity to the metal chelating

10.1002/chem.201702647

center in our previous α-amino acid analogs leading to diminishing of transporter recognition as bulkiness increased. Additionally, the crystallographic data indicate the presence of two sets of H-bonding network dominating the recognition event.[22b, 23] The first H-bonding network links between the hydroxamate oxygens and proton-donors within the transporter; while the second network connects the ring backbone in FC with the transporter. Keeping α position unsubstituted and introducing moieties capable of hydrogen bonding were expected to expend the number of biologically active FC analogs. Thus, replacing α-amino acid hydroxamates with their β and γ equivalents tackles both complementary approaches simultaneously: introducing polar substituents for enhanced hydrogen bonding to the transporter, yet moving them further away from the metal binding site. A recent example of analogs with β positioned hydroxamates[24] indicates a significant potential of this approach.

In this paper, we present a new series of improved FC analogs. The series comprises eight new tripodal iron complexes, designed to incorporate a number of variable structural elements in order to investigate their influence on physico-chemical properties, as well as on their microbial uptake process. In terms of iron affinity, the pFe[25] values of most analogs are within the range of typical siderophores. However, in terms of siderophore activity more variability is observed: from a rare case of species-specificity to a broad-spectrum activity similar to native FC. While the first may find application in bacterial diagnostics the second, with the broad-spectrum activity, may offer future therapeutic advantages.

Fluorescently marked broad-activity analog was followed in several mutants of FC transport cascade in *E. coli* and its pathway proved to be indistinguishable from that of FC, thus making it a 'truly' biomimetic analog. Same fluorescently labeled analog provided a real-time imaging tool for distribution patterns inside bacteria and fungi subsequent to iron uptake. These images describe quite different 'trafficking' and compartmentalization, identify discrete targets and suggest utilization of diverse drug-conjugates for differential activities.

We also show that our most versatile FC analog attached to Quantum Dots (QD) generates an adhesive and emissive platform ready for tethering microorganisms possessing the FC transporter. Coupled with other siderophores or their analogs, this platform carries the potential to overcome the formidable need to find distinct growth conditions for difficult-to-culture microorganisms. The QD derived methodology allows 'fishing' bacteria, based on siderophore content, thus providing rapid means for potential microbial diagnostics and separation.

Taken together the presented results not only shed light on the insufficiently studied fate of siderophores subsequent to iron delivery, but also provide a tool for identifying new therapeutic targets, distinct for different microorganisms.

Results and Discussion

Design and synthesis. In the current series of FC analogs two sets of compounds derived from β- and γ- amino acids were prepared; one containing long unsubstituted arms similar to those in FC, while the other contains chiral centers and possesses peripheral functional groups.

Detailed structures of all the analogs in this series are provided in Chart 1. The simplest β-amino acid, β-alanine, and the simplest γ-amino acid, γ-aminobutyric acid (GABA), yielded the structural skeleton of the series represented by analogs **1** and **2** respectively. Utilization of natural aspartic and glutamic amino acids led to chiral structures with peripheral carboxylates (analogs **3** and **4**). A non-natural chiral amino acid, homo-β-alanine, incorporates a methyl group instead of a carboxylate at the β position to the hydroxamate (analog **5**). Replacement of carboxylates by methyl groups allows the comparison of steric effects at the β position in homo-β-alanine derived tripod **5** to steric and electrostatic effects of the carboxylates in aspartic derived tripod **3**. All chiral analogs (**3**-**5**) were prepared as a pair of enantiopure compounds.

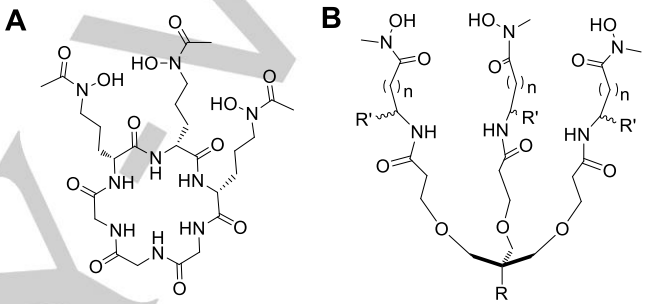

Chart 1. Structures of FC and its β- and γ- amino acid biomimetic analogs: [A] Structure of the native FC. [B] Schematic representation of the biomimetic FC analogs. Analog **1** is derived from β-alanine amino acid, R=NH_2, R'=H, n=1; Analog **2** - GABA amino acid, R=Me, R'=H, n=2; Analog **3**- aspartic amino acid, R=Me, R'= COOH, n=1; Analog **4**- glutamic amino acid, R=Me, R'=COOH, n=2: Analog **5**- homo-β-alanine amino acid, R=Me, R'=Me, n=1.

Most analogs in the series were prepared by a convergent synthetic route combining three building blocks (Scheme 1). First, the templates were assembled by reacting triols **6** or **7** with tert-Butyl acrylate. When triol **7** was utilized, the apical amine was protected with Alloc prior to hydrolysis of the t-Butyl esters, which yields the deprotected triacids **12** and **13**. The second building block, namely *N*-methyl *O*-benzylhydroxylamine hydrochloride **18** was prepared as described elsewhere.[26] Next, it was coupled to commercially available *N*-Boc protected amino acids **14**-**17** using CDI to obtain the protected arms **19**-**22**. After Boc removal these arms were coupled to a suitable template to obtain *O*-Benzyl protected tripods **27** and **29**-**31**. Hydroxamic acids were finally deprotected using hydrogenolysis to yield the final analogs **1**-**3** and **5**. When triacid **12** was utilized Alloc was removed prior to hydrogenolysis (compound **28**).

The convergent synthetic route failed in the case of analog **4**. The coupling step between the corresponding deprotected arm

10.1002/chem.201702647

Scheme 1. Convergent synthetic route to FC tripodal analogs:

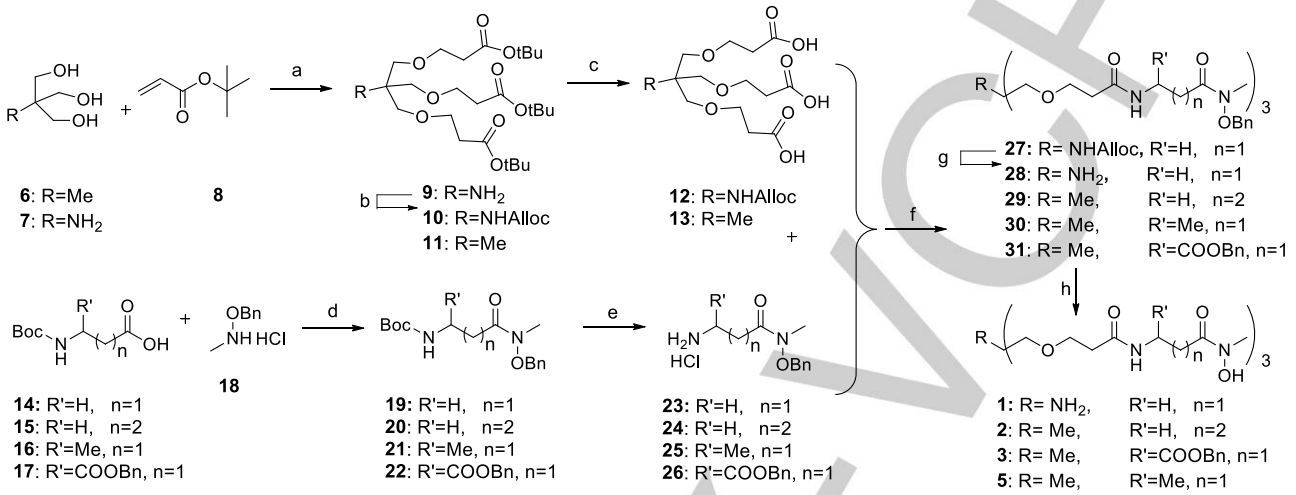

Reagents and conditions: (a) $NaOH_{aq}$, TBAI; (b) Allyl chloroformate, NaOH (aq.), THF, 0° C→r.t.; (c) 4N HCl in dioxane; (d) CDI, DIPEA, THF; (e) 4N HCl in dioxane, 0°C; (f) CDI, DIPEA, THF; (g) 1.2 mol% $Pd[Ph_3P]$, $PhSiH_3$, DCM; (h) H_2, Pd/C, MeOH.

and triacid **13** led to intramolecular cyclization, forming a pyroglutamic acid derivative instead of the desired tripod. Thus, this analog was obtained by a linear synthetic route (Scheme 2) starting from previously described glutamic acid derivative **32** with γ-carboxylate protected by trimethylsilyl ethanol (TMSE). After coupling to template **13** TMSE was removed by TBAF to yield triacid **34**, which was immediately coupled to hydroxylamine **18** using CDI to obtain the benzyl protected tripod **35**. Finally, the benzyl groups were removed by hydrogenolysis to yield the desired analog **4**.

Scheme 2. Linear synthetic route to glutamic acid derived analog 4.

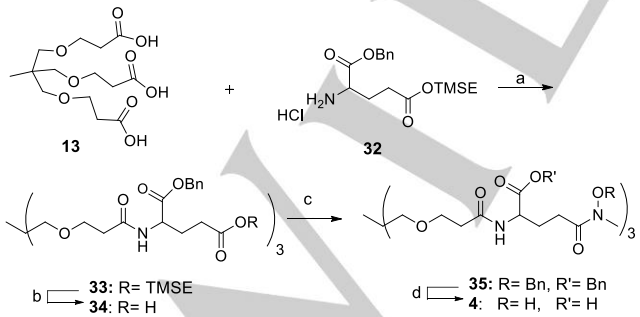

Reagents and conditions: (a) CDI, DIPEA, THF; (b) 1N TBAF in THF; (c) hydroxylamine **18**, CDI, DIPEA, THF; (d) H_2, Pd/C, MeOH.

For additional studies analog **1** was either loaded CdSe/CdS/CdZnS/ZnS QDs (Scheme 3) or labeled wit naphthalimide fluorescent dye **42** (Scheme 4). Synthesis of QD conjugate began from fully protected β-alanine derived tri **27**.

Scheme 3. Conjugation of β-alanine derived analog to CdSe/CdS QDs.

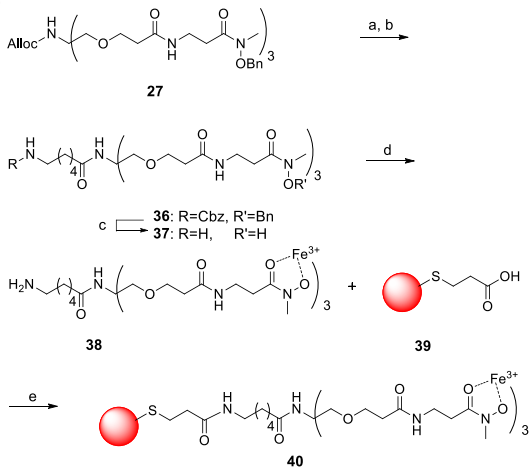

Reagents and conditions: (a) 1.2 mol% $Pd[Ph_3P]$, $PhSiH_3$, DCM; (b) NHS, DIC, DIPEA, THF. Yield: 66% for two steps; (c) H_2, Pd/C, MeOH. Quant. yield; (d) 1 eq Fe^{3+}, MeOH. Quant. yield; (e) EDC, KOH, H_2O/MeOH.

10.1002/chem.201702647

Scheme 4. Labeling of β-alanine derived analog with a naphthalimide fluorescent dye.

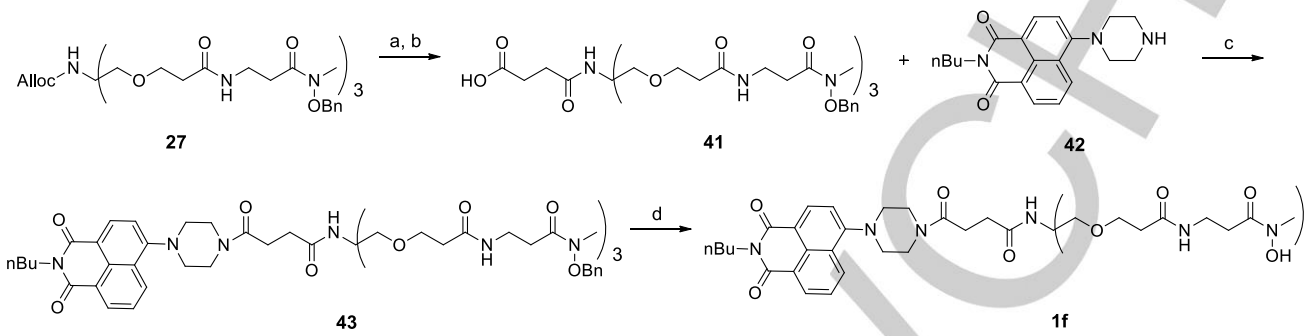

Reagents and conditions: (a) 1.2 mol% Pd[Ph_3P], $PhSiH_3$, DCM; (b) Succinic anhydride, TEA, THF; (c) HBTU, DIPEA, DCM: DMF 1:1; (d) H_2, Pd/C, MeOH.

Following Alloc removal it was coupled to *N*-Cbz protected caproic acid, thus introducing a flexible linker in order to separate between the analog and the QDs' surface. The obtained intermediate **36** was subjected to hydrogenolysis to remove protection from both the hydroxamic acids and the terminal amine (compound **37**). Next, the free hydroxamic acids were complexed with ferric chloride (intermediate **38**). The iron complex served as a protecting group for hydroxamic acids and later was used for further experiments with bacteria. Finally, the iron complex **38** was loaded on the QDs by coupling its terminal amine to multiple carboxylates on the surface of each particle to obtain β-alanyl tripod decorated QDs (Compound **40**).

Fluorescent labeling of β-alanine derived analog (Scheme 4) started from deprotecting the apical amine of compound **27**. This amine was further reacted with succinic anhydride to introduce a short linker for dye connection (compound **41**). The carboxylate of the linker was coupled to the piperazine of the previously reported dye **42**.[27] Finally, the labeled analog **1f** was obtained after deprotection of **43** by hydrogenolysis.

Overall Iron Complex Stability. Successful biomimetic compounds must efficiently perform the function of the natural entity they mimic. Siderophores encapsulate the ferric ion with extraordinary affinity in order to overcome extremely low soluble iron concentrations in the natural environment.[28] Thus, determination of iron complex stabilities of siderophore biomimetics is vital for their application under natural iron concentrations and competition with other siderophores.

Results of physico-chemical analysis are summarized below and in Supporting Information. All tripodal compounds form mononuclear complexes with ferric ions, and the metal-to-ligand 1:1 stoichiometry was confirmed by ESI-MS (Table S2) and spectrophotometry (vide infra).

In order to determine the stability constants of the trihydroxamate forms of discussed ferric complexes, FeL_1- FeL_5 (analogs **1**-**5**), the spectrophotometric competition experiments with EDTA were performed at pH 8.0. The overall stability constants, logK_{FeL} (Table 1), were calculated according to eq. S6, and using known values of protonation constants of respec ligands (Table S1), EDTA and stability constant of Fe-EDT For analogs **3** and **4** some instability of the ferric complexes observed before the equilibrium with EDTA could be attai and the constants were not reliable (not shown). Therefore, development of different method was necessary. A combina of pH-dependent spectrophotometric and potentiom titrations was applied. The logK_{FeL} are given in Table 1. C values of logK_{FeL} of analogs **2** and **5** determined by E competition experiments and pH-depen spectrophotometric/potentiometric titrations (Table 1) indi the reliability of the second method.

Table 1: Overall stability constants (logK_{FeL}) and pFe values for st complexes with iron (III) ions[a]

Analog	logK_{FeL}	pFe
1	26.20(5)	23.3
2	28.7(2)[b] 28.05(1)	23.7
3	24.4(1)	17.2
4	24.65(9)	19.8
5	27.8(2)[b] 27.06(3)	23.3
FC	29.07[c]	25.2[c]

[a] Conditions: T = 298K, I = 0.10M $NaClO_4$. [b] Constants determined EDTA competition titration. Conditions: $c_{lig} = c_{Fe}^{III} = 1.5 \cdot 10^{-4}$M, c_{EDTA} = 0-1. ^{3}M, I = 0.10M $NaClO_4$. [c] Reference.[30]

In order to eliminate the differences in ligand protonation constants, which may influence logK_{FeL}, and compare the iron chelation efficacy between the studied ligands, and parental FC, the free hexa-aqua-iron(III) concentrations were calculated (pFe = -log[Fe^{III}(aq)] at pH = 7.4 with a total ligand concentration of 10^{-5} M and total Fe^{III} concentration of 10^{-6} M, Table 1).[25, 31]

Comparison of all obtained data reveals that the pFe values obtained for analogs **1**, **2** and **5** are very close, while these of carboxylate derivatives **3** and **4** are significantly lower. The analysis of pH-dependent UV-visible spectral profiles of all compounds exposes an influence of the carboxylates on the trihydroxamate complex formation. The pH-dependent spectral characteristics of the ferric-analog **1**, **2** and **5** systems clearly indicate the presence of only two absorbing species along the pH range studied (0.1-8), i.e. dihydroxamate[32] and trihydroxamate (Plot S1, Table S4), with equilibria between the two forms, represented as pK_{NHOH}, ranging from 2.45 for **2** to 2.76 for **5** (Table S3). This weak difference indicates that shortening of the spacer between the hydroxamate group and the amide moiety, or the presence of uncharged methyl group nearby the hydroxamate only very slightly affect the binding properties of the molecule. Presence of the carboxylate in close proximity to the hydroxamate hampered the binding of third hydroxamate group, with the pK_{NHOH} of 7.3 and 6.75 for **3** and **4**, respectively (Table S3). Likely, one of the carboxylate groups is involved in complex formation along with two hydroxamates. Only after the deprotonation of the third hydroxamic group, trihydroxamate complex formation is possible. The tridentate coordination via hydroxamate and carboxylate oxygens was earlier documented for iron(III) complexes of aspartic acid-β- and glutamic acid-γ-hydroxamic acids.[33] In these sytems the preferential binding of carboxylate in complexes of 1:1 and 1:2 Fe^{III}:ligand stoichiometry prevented the formation of complexes with 1:3 ratio, typical for monohydroxamates. In addition, when unbound the carboxylates might destabilize the ferric complexes through induction of electrostatic repulsion and/or steric constrains.

Overall, the pFe values calculated for analogs **1**, **2** and **5** are less than two orders of magnitude lower than of FC. However, pFe of analogs with carboxylate groups (**3** and **4**) are up to eight orders of magnitude lower, indicating a destabilizing role of carboxylates in encapsulation of ferric ions by the hydroxamates. It is worth emphasizing that at pH 7.4, there are still mixed carboxylate-hydroxamate complexes present (Plot S4). Nevertheless, pFe values for all studied tripodal FC analogs remain in the range for effective iron chelators.

Bacterial growth promotion studies. The ability of iron-loaded analogs **1**-Fe^{III} - **5**-Fe^{III} (Table 2) to serve as a sole iron source for bacteria was quantified as growth level in iron-depleted MKB medium. To eliminate background iron, the medium was treated with an iron chelating amidoxime resin 'Purolite S910' ("Purolite"). Two bacterial strains were used in this study: *E. coli* UT5600[34] and *P. putida* JM218.[19a] Both strains are defective in siderophore production in order to exclude the possibility of iron uptake through the action of naturally secreted siderophores. Thus, iron complexes of the analogs were added as a sole iron source and growth levels were measured over time until the stationary phase. To ensure equal amount of added iron source, stock solutions of all analogs were calibrated using the Cu·CAS method.[35] Iron complex of native FC was used as a positive control and represents the maximal growth level in each experiment. Sterile double distilled water, instead of an iron source, was used as a negative control. Each enantiomer of chiral analogs **3**-**5** was tested separately. Table 2 presents the results as relative growth promotion activity. Actual growth curves are presented in the Supporting information (Figure S2). All tested analogs demonstrated growth promotion activity at least in one bacterial species and the majority of the tripods were recognized by both bacterial strains used in this study. Overall, *P. putida* was less selective and was able to take advantage of more analogs than *E. coli*, although both species perfectly recognize the native FC. Notably, b enantiomers of chiral analogs **3**-**5** had similar growth promo and no chiral preference was observed in either of the bacte strains.

The majority of native siderophores incorporate cl building blocks, frequently derived from amino acids Consequently, the asymmetric centers of the ligand also di the chirality of the octahedral iron(III) complex, which ad either Λ or Δ arrangement around the ferric ion, since the configurations become energetically nonequivalent. The o membrane receptor selectively recognizes and transports complexes of predominantly one configuration.[37] In the cas FC its outer receptor is built to recognize the Λ arrangen around the iron, induced by its L-ornithine derived arms.[38]

Table 2: Bacterial growth promotion of the FC tripodal analogs in the cu series.

Iron sources	Amino acid [a]	Relative growth promotion	
		E. coli	*P. putida*
FC- Fe^{III}		++++	++++
1 - Fe^{III}	β-alanine	++++	++++
2- Fe^{III}	GABA	+	++++
3- Fe^{III} [b]	aspartic acid	++	++
4- Fe^{III} [b]	glutamic acid	++	+++
5- Fe^{III} [b]	h- β-alanine	-	++++
DDW		-	-

Relative growth promotion activity levels: ++++ full activity comparable to +++ high activity; ++ moderate activity; + weak activity; - no activity. ferrichrome, DDW - Double Distilled Water; [a] amino acid incorporated int iron binding arm of each analog, [b]both enantiomers promote equal gr levels in both strains. Actual growth curves are presented in the Suppo information (Figure S2).

Iron complexes of achiral siderophores, such as desferrioxamine (DFO), exist as a racemic mixture of Λ and Δ enantiomers.[39] However, unlike carbon-generated asymmetric centers, Λ and Δ configurations are in dynamic equilibrium and

can interchange. The receptor still recognizes mainly one structure, but it also shifts the equilibrium towards the uptaken form. Subsequently, given enough time the whole population of the siderophore can be utilized. Current series of FC analogs comprises two achiral compounds, namely β-alanine derived tripod **1** and GABA derived tripod **2**, as well as three chiral analogs derived from aspartic acid (tripod **3**), glutamic acid (tripod **4**) and homo- β-alanine (tripod **5**). Bacterial growth studies (Table 2) demonstrated equal siderophore activity for both enantiomers of each chiral analog. Circular Dichroism (CD) spectroscopy provided a plausible explanation for these results. While enantiomers of β-amino acid, tripods **3** and **5**, display a distinct chirality pattern around the iron, for γ- amino acid analog **4** at the same concentration only a trace signal was observed in the Ligand to Metal Charge Transfer (LMCT) region of the iron complex (data not shown).[14d] Such decrease in chiral preference around the iron with increasing linker length has been previously observed in transition from α to β oriented hydroxamates as well.[24] The chiral center of β and γ amino acids is decoupled from the hydroxamates by one or two methylene spacers. As a result, the existing chiral center cannot induce a strong chiral preference around the bound iron, like in native siderophores, and both enantiomers of each analog can be recognized by the outer membrane receptor, probably through the equilibrium exchange between the Λ and Δ configurations. For practical applications of β- and γ- amino acid derived tripods the chirality of the utilized amino acid does not seem to play significant role in bacterial recognition and both enantiomers are probably useful in the preparation of biologically active analogs.

Using artificial mimics, it is possible to compare between bacteria in terms of selectivity for iron sources. FC is recognized to the same extent by both species in this study. However, comparison between the biomimetic analogs reveals hidden differences, and finer organization levels of their iron uptake systems become visible. While *P. putida* can recognize practically any tris-hydroxamate ferric complex in the current series, *E. coli* is more selective and sensitive to sterical hindrance, even at the β-position to the iron binding site. This is demonstrated by comparison between β-alanine and homo-β-alanine derived tripods **1** and **5**. While the former is fully recognized by *E. coli*, one methyl at the β-position of the latter switches off the recognition. In light of this result, the moderate siderophore activity of the aspartic derived tripod **3** in *E. coli* comes as a surprise, because this tripod has a carboxylate at the β-position. In terms of sterical hindrance this functional group has a more dramatic effect, yet *E. coli* still recognizes it as a suitable iron source to a significant extent. *P. putida* behaves differently towards analogs, which contain carboxylates. Both tripods **3** and **4** demonstrate lower growth promotion in this strain compared to other compounds in the series. The effect of polar side groups at various positions relative to hydroxamates should be further examined by constructing additional analogs.

E. coli is demanding not only in terms of sterical hindrance, but also in the number methylenes separating the template bound amides and the hydroxamic acids. We have previously established that the glycine derived tripod with one methylene spacer was not recognized by *E. coli*. On the other hand, tripod **1** with two-methylene spacer had excellent growth promotion activity, while analog **2** with three methylenes was only weakly active. Therefore, in the given series *E. coli* demonstrates optimal uptake for two methylene spacer arms. Yet again, the addition of a carboxylate, this time to the γ-amino acid skeleton (glutamic derived analog **4**), had a positive effect on the recognition process in *E. coli*.

Two main structural parameters seem to control FC ana recognition by *E. coli*: (i) presence of substituents on the chelating arms, (ii) linker length connecting the template to hydroxamates. Generally, substituents interfere with recogniti except for carboxylates, which might play a role in hydro bonding to the FhuA transporter. On the other hand, the lir length has an optimum at two methylenes (analog **1**). Follov these guidelines leads to broad-spectrum activity (analog Disregarding them results in species-specificity towards *putida* (analog **5**).

β-alanine derived tripod **1** showed superior gro promotion in both tested strains. To follow its distribution a iron uptake it was labeled with naphthalimide dye **42**. This dy quenched in the presence of iron and lights up only in the chelator. Therefore, it is used as a turn-on sensor for extraction from siderophores. Both *E. coli* and *P. putida* v incubated with the iron complex of the labeled analog **1f** several minutes and observed using fluorescent microsc Figure 1A demonstrates a typical result of such experiment. A iron uptake, the green fluorescence of the free chelato concentrates in the periphery of the bacterial cell, while cytosol remains darker. Thus, secretion of the free analog f the cytosol after iron extraction is probably a fast process. experiment demonstrated in Figure 1A does not provide eno information about the exact location of the secreted analog 1 could theoretically reside in the periplasmic space or bin bacterial cells from outside. An elegant solution, which all distinguishing between the two possibilities, was found literature. It was previously reported that in gram-negative under osmotic stress the cytosol shrinks and the peripla deforms and relocates to the opposite poles of the cell.[40] W osmotic stress was induced by adding glycerol to live bact cells, incubated with iron complex of **1f** the fluoresce relocation was consistent with this of the periplasmic space was clearly observed in the two poles of both *E. coli* and *P. pu* strains (Figure 1B, *E. coli* demonstrated similar results). Thus, after iron extraction the free chelator is rapidly excreted to the periplasmic space and remains there for a significant amount of time. These findings are in line with a report on antimicrobial activity in gram-negative bacteria of a hydroxamate-type siderophore, conjugated to a β-lactam antibiotic.[41] Alternatively, it might be reasonable to target both membranes of gram-

negative bacteria from within the periplasmic space through conjugation with surface active compounds, e.g. antimicrobial peptides.

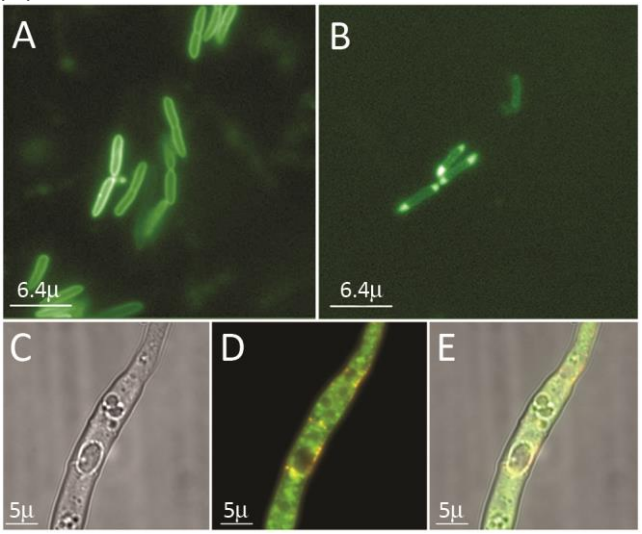

Figure 1. Distribution of analog 1f in bacteria and fungi following microbial iron uptake from the supplied 1f-Fe^{III} complex: Analog **1f** is quenched by iron and becomes fluorescent upon iron extraction by bacteria or fungi. [A] Distribution pattern in live *P. putida*. The fluorescence of the iron-free analog concentrates in the periphery of the bacterial cells. [B] Osmotic shock was induced in *P. putida*, incubated with iron-loaded tripod **1f**. The fluorescence shifts to the poles of the bacterial cell, consistent with the periplasmic space translocation under osmotic shock. [C-E] Light and fluorescence images of the fungus *U. maydis*, labeled with FM4-64 membrane dye and incubated with analog **1f**. [C] DIC image. [D] two-channel fluorescence image: green- analog **1f**, orange-red- FM4-64. Iron free analog **1f** is mostly present outside the labeled vesicles and its internalization is consistent with the uptake mechanism of native FC. [E] merge of DIC and fluorescence images.

In gram-negative bacteria iron loaded siderophores are transported into the cell via a chain of specific receptors.[4a, 42] In the case of FC uptake in *E. coli,*[4c, 43] iron loaded FC is first recognized by the outer membrane receptor FhuA, which transports it into the periplasmic space using the proton motive force, supplied by TonB.[44] In the periplasm the siderophore-iron complex binds to the FhuD shuttle protein. FhuD brings it to the inner membrane receptor FhuB, which transfers the iron complex across the cytoplasmic membrane, using energy provided by the adjacent ATPase FhuC.[45] We were interested to estimate whether the iron complex of β-alanyl derived analog **1f** enters the bacterial cell via the same pathway as FC. Thus, we repeated the fluorescence microscopy experiment with several *E. coli* knockouts, each lacking a component of the FC uptake system, namely deletion mutants: ΔfhuA,[9] ΔtonB, ΔfhuD, ΔfhuB and ΔfhuC (the Keio collection)[46]. After several minutes of incubation with **1f**-Fe^{III} fluorescence was monitored in each strain and compared to that of *E. coli* ΔentC,[46] which has intact FC uptake system. In all but one mutant no fluorescence could be detected. In ΔfhuB strain residual fluorescence could be observed, consistent with the possibility of partial iron extraction in the periplasm, described in literature.[37] These results emphasize the necessity of all FC uptake system components for efficient processing of **1f**-Fe^{III} by *E. coli.* Using a suitable 'cascade of mutants' we were able to demonstrate that compound **1f**-Fe^{III} utilizes the same pathway as the iron-loaded FC, making the β-alanyl tripod a 'truly' biomimetic analog.

FC is an endogenous siderophore to many fungal species, including the extensively studied *Ustilago maydis*.[47] In fungi two distinct mechanisms of iron acquisition from siderophores exist. Some siderophores donate their iron at the membrane with entering the cell, while others are actively transported into cytoplasm along with the ferric ion. FC is known to internalized via the active transport mechanism.[36]
U. maydis was incubated with **1f**-Fe^{III} (Figure 1C-E). W minutes, intense green fluorescence of the free chelator c be observed in the cytosol (Figure 1D). Therefore, the complex of β-alanine derived analog is efficiently recognize *U. maydis* and is transported to the cytoplasm, similarly to na FC. Membrane dye FM4-64[48] (Figure 1D, orange-red) added as well to follow vesicle trafficking. Analog **1f** is distribu mostly outside the labeled vesicles and displays a punc pattern.

Overall, fluorescence microscopy results in *P. putida coli* and *U. maydis* emphasize the cross-phylum siderop activity of β-alanyl derived analog, similarly to native Previously, another tripodal FC analog displayed uptake utilization by *U. maydis*.[49] However, it could not be recogni by *E. coli*, thus diverging from native FC.

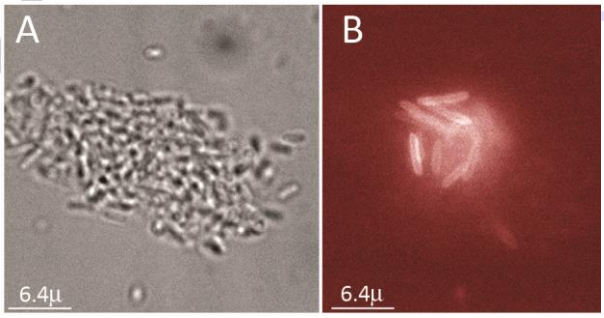

Figure 2. Bacterial cluster formed around emissive QDs coated with iron-loaded β-alanyl derived analog: [A] Bright field image of a bac aggregate formed after application of the coated QDs. [B] Fluorescence in of the bacterial cluster. Red emission is observed from within the bac aggregate.

Due to the highly stabile association between siderophores and their outer-membrane transporters, it is possible to capture microorganisms by immobilized siderophores. Given the vast assortment of available siderophores and their analogs they can be used for differentiation between microorganisms and for

pathogen detection. Indeed, in recent years such prototype systems were built using chips, functionalized silica and even gold nanoparticles.[50]

Iron complex of β-alanine derived analog **1** was bound to emissive QDs in order to examine the possibility of bacterial trapping on their surface. To ensure proper interactions between the analog and its outer membrane receptor, a long flexible linker was introduced between the tripod and the surface of the QDs. The iron complex decorated QDs were incubated with bacteria, grown under iron starvation. Figure 2A shows a bright field image of a bacterial aggregate formed after several minutes. Unlike the naphthalimide fluorescent label **42**, these particular QDs are not quenched by iron. The fluorescence image of the same cluster (Figure 2B) clearly shows the QDs fluorescence, which is emitted from within the bacterial cluster. Such cluster formation behavior could lead to development of bacterial cell concentration methods, using various siderophore analogs. Species-specific artificial analogs could play a crucial role in development of methodologies for selective bacterial concentration from diluted samples, especially when culturability issues arise. Emissive QDs are readily available in a wide range of colors. Coated each with a different analog or a native siderophore, such array could provide a platform for microbial separation based on diversity of their iron uptake systems.

Conclusions

This work addresses itself to identify structural motifs in FC mimics that control siderophore activity. This paper describes a series of biomimetic analogs to FC designed to identify structural motifs governing broad-spectrum activity on one hand and promoting species-specificity on the other. A set of guidelines to both effects have been formulated and discussed. The major contribution to obtaining additional structurally diverse analogs came from utilization of β- and λ- amino acid derived hydroxamates.

Growth promotion activity of the current mimics presented a dramatic variation, from an analog specific exclusively to *P. putida*, but not to *E. coli* (tripod **5**) to an analog with FC-like activity causing maximal growth promotion in both *E. coli* and *P. putida* (tripod **1**). Other analogs fall in between, exhibiting some activity in both strains (tripods **2**-**4**). No difference in activity could be observed in enantiomers of analogs **3**-**5**, most probably due to weak induction of chiral preference around the iron by the β- and γ- positioned chiral center.

Although different analogs vary in iron binding efficiency over a substantial pFe range, all of them fall within the active siderophore values. Correspondingly, these data emphasize the unfavorable influence of carboxylate substituents on iron affinity (analogs **3** and **4**), probably due to combination of electrostatic repulsion and competition with hydroxamates over ferric ion coordination. Due to beneficial effect of carboxylate substituents on siderophore activity in the case of *E. coli*, it might be interesting to examine additional analogs with polar, but not charged or chelating groups.

Attaching a fluorescent tag to the analog most similar to FC (tripod **1**) enabled following its fate post iron utilization in real-time. While in *P. putida* and *E. coli* the periplasmic space was identified as the cellular destination and the site of accumulation for the iron-free analog, in *U. maydis*, cellular targets within the cytosol were visualized and recorded. These results also emphasize the biomimetic nature of analog **1f,** acting cross phylum, like native FC. Furthermore, tripod **1f** utilizes the uptake pathway of FC as demonstrated by FC transport mutants i *coli*. Coupled with high iron affinity, these data mark the alanine derived tripod a 'true' biomimetic FC analog.

Emissive QDs provided both fluorescence and a surf for coating with multiple molecules of analog **1** iron complex. surface proved to be well suited for immobilization of recognizing bacteria. Such bacterial clusters, formed aro QDs, might provide a platform for future bacterial selection concentration, based on siderophore diversity. This could especially useful in cases of impaired culturability. Diffe siderophores or their analogs, coupled to a palette of emis QDs might be applicable in various sorting techniques.

The power of biomimetic chemistry is clearly demonstra in mimicking FC by starting with simplified structures. Only a reiteration steps were sufficient to reach maturity and ob mimics that fulfill all the functions reserved to native FC. On way, FC mimics with unique properties were identified leadin remarkable abilities awaiting utilization. The biomim approach is not limited to a given initial structure and there other starting templates and their reiteration, modifications proper tune-up should equally be expected to reach sin results and mimics with new capabilities collected on the roa

The chemical versatility allows starting with modi structures ready to induce additional functionalization combination of elementary properties like 'recognition' 'signaling' capabilities, described in the second part of manuscript, resulted in obtaining an arsenal of theoretical practical tools for visualizing iron 'trafficking' compartmentalization, thus distinguishing between bacteria fungi. In general, this methodology allows mapping addressable targets. Iron transporters are solely reserved to microbial world while mammalian cells resort to entirely diffe mechanisms for their iron supply. A long sought antifungal ag that does not interact with mammalian cells, primarily of live kidneys, due to their lack of siderophore transporters, seen likely outcome worth perusing.

Experimental Section

Materials and methods. Commercially available amino acids, coupling and protecting group reagents were purchased from "ChemImpex international". Other fine chemicals were purchased from "Sigma Aldrich".

Amidoxime iron (III) chelating resin Purolite® S910 was obtained from Purolite® SRL. Magnesium sulfate heptahydrate for the preparation of MKB medium of Bio Ultra grade (min. 99.5%) was purchased from Sigma Aldrich. Commercial reagents were used for synthesis without further purification. Flash chromatography was performed using "Merck" Kieselgel (40-63 µm) silica gel. NMR spectra were recorded on "Brucker Avance" 250 MHz, 300 MHz, 400 MHz and 500 MHz machines equipped with QNP probe. Chemical shifts are reported in ppm on the δ scale downfield from TMS. ESI-MS spectra of synthetic intermediates were recorded in a ZQ-4000 ("Micromass", Manchester, UK) instrument. Bacterial growth was measured using a BioMate-3 spectrophotometer ('Thermo Electron Corporation', Wisconsin US). For physico-chemical studies all solutions were prepared in doubly distilled water. Water was de-oxygenated by CO_2- and O_2-free argon. All stock solutions were prepared using a R200D Sartorius analytical balance (precision 0.01 mg). Iron(III) perchlorate stock solution was prepared immediately before use from $Fe(ClO_4)_3 \cdot xH_2O$ ('Aldrich', chlorides < 0.005%) in 0.01 M $HClO_4$ (AppliChem p.a. 70%) and standardized by ICP-AES. $HClO_4$ solution was titrated by standardized NaOH (0.1 M 'Fluka' standard solution). Carbonate-free NaOH solution (0.1 M 'Fluka' standard solution) was standardized by titration with potassium hydrogen phthalate ('Merck'. p.a.). For detailed synthetic procedures and characterization (^{1}H-NMR, ^{13}C-NMR and ESI-MS) of all new compounds please refer to the Supporting information. Selected examples are presented below.

Amine tripod 28: In a three-necked round bottom flask tripod **27** (0.64 g, 0.64 mmol) was dissolved in dry DCM (10 mL). The flask was sealed with a rubber septum and phenylsilane (160 µL, 1.28 mmol, 2eq) was added through. The reaction mixture was degassed by bubbling dry nitrogen gas into the reaction mixture while vigorously stirring for 10 minutes. Next, tetrakis(triphenylphosphine)palladium(0) (15 mg, 2% W/W) dispersed in DCM (1 mL) was added to the flask and degassing continued for additional 10 minutes. Nitrogen stream was closed and the reaction mixture was stirred in the dark for 2 hrs. Once the reaction was complete (followed by TLC with ninhydrin staining) solids were filtered off and volatiles were evaporated. Final purification was performed using silica gel chromatography with EtOAc: MeOH (9:1) as eluent to yield the desired product as viscous colorless oil (0.55 g, 95% yield). ^{1}H-NMR (300 MHz, $CDCl_3$): δ 2.40 (t, *J* = 5.7 Hz, 6H), 2.60 (bt, *J* = 5.3 Hz, 6H), 3.17 (s, 9H), 3.38 (s, 6H), 3.48 (dd, *J*1=11.7 Hz, *J*2=5.7 Hz, 6H), 3.66 (t, *J*= 5.7 Hz, 6H), 4.79 (s, 6H), 7.02 (bs, 3H), 7.36 (m, 15H). ^{13}C-NMR (300 MHz, $CDCl_3$): δ 32.13, 33.32, 34.49, 36.86, 55.98, 67.41, 72.55, 76.18, 128.85, 129.19, 129.42, 134.07, 171.29, 173.88. ESI-MS: calc.: 907.47, found: 907.59.

Protected caproic acid linked tripod 36: Cbz protected 6-aminohexanoic acid (105 mg, 0.4 mmol) was dissolved in DCM (3 mL), and stirred at RT for a few minutes. *N*-hydroxysuccinimide (55 mg, 1.2 eq) was dissolved in THF (2 mL) and added to the reaction mixture. pH of the reaction was brought to alkaline using DIPEA, followed by addition of DIC (130 µL, 2.1 eq). The mixture was left to stir for 3 hrs at RT. Compound **28** (152 mg, 0.3 mmol) was added and the reaction was stirred at RT for 24 hrs. All volatiles were evaporated and the crude was dissolved in EtOAc. The solution was kept in -18 °C for a few hours and the white precipitate was filtered off. The organic layer was washed with 1N HCl x3, followed by water, 5% $NaHCO_3$(aq) x3 and brine. The resulting organic layer was dried over Na_2SO_4, and the solvent was evaporated. The residue was adsorbed to silica and loaded onto a silica gel column, equilibrated with Hex: Acetone (9:1); the final product was eluted with a gradient of Hex: Acetone (9:1 to 8:2). The product was obtained as a white solid (200 mg, 57%). ^{1}H NMR (400 MHz, $CDCl_3$) δ 1.33 (quint, *J* = 6.7 Hz, 2H), 1.49 (quint, *J* = 7.0 Hz, 2H), 1.58 (quint, *J* = 7.1Hz, 2H), 2.18 (t, *J* = 7.1 Hz, 2H), 2.37 (t, *J* = 5.6, Hz, 6H), 2.60 (bs, 6H), 3.18 (m, 11H), 3.47 (d, *J* = 5.5 Hz, 6H), 3.64 (t, *J* = 5.6Hz, 6H), 3.70 (s, 6H), 4.80 (s, 6H), 5.07 (s, 2H), 5.23 (bs, 1H), 6.49 (s, 1H), 6.91 (bs, 3H), 7.37 (m, 20H). ^{13}C DEPTQ NMR (400 MHz, $CDCl_3$) δ 25.10, 26.11, 29.49, 32.21, 33.35, 34.52, 36.61, 36.80, 40.82, 59.71, 66.43, 67.34, 69.20, 76.24, 127.96, 128.03, 128.43, 128.72, 129.07, 129.28, 134.08, 136.72, 156.46, 171.26, 173.61, 173.82. ESI-MS: calc.: 1154.59, found: 1154.99.

Coupling of tripod 38 to QDs: CdSe/CdS/CdZnS/ZnS QDs were fabricated by Successive Ionic Layer Adsorption and Reaction (SIL method.[51] The QDs were coated with 3-Mercaptopropionic acid (M to provide surface carboxylates for coupling to tripod **38**, each QD ha about 400 carboxylates on average. Carboxylate coated QDs were k provided by Prof. U. Banin from the Hebrew University in Jerusalem storage, QDs were divided to aliquots (1x10^{-9} mol each), two volume acetone were added to each aliquot, precipitated QDs were span d by centrifugation (6500 rpm, 2 min) and the solvent was discarded. QD pellet was stored at -20 °C. Protected tripod **36** (80 mg, 0.07 m was dissolved in MeOH (10 mL), Pd cat. (10% on carbon, 10 mg) added and the reaction was stirred for 4.5 hrs under hydro atmosphere. Pd was filtered off, and MeOH was evaporated to pro the final deprotected compound **37** (48 mg, 99%), which was immedi used. To HEPES buffer (10 mM, pH=7.4, 240 µL) tripod **37** (0.02 MeOH, 30 µL) was added, followed by ferric chloride (0.02M in Me 30 µL, 1 eq) to form the stock solution of iron complex **38**. QDs (1x mol) were reconstituted in HEPES buffer (10 mM, pH=7.4, 250 containing EDC (10 mM) and incubated for a few minutes. Stock solu of **38** (10 µL, 20 eq) was added to the activated QDs and the rea mixture was shaken for 1 hr. Excess reagents were separated functionalized QDs **40** by dialysis against DDW.

Protected naphthalimide tripod 43: Tripod **41** (403 mg, 0.4 mmol) dissolved in DCM:DMF (1:1, 5 mL) and cooled on an ice bath. A few d of DIPEA were added to bring the pH to around 7. HBTU (350 mg, mmol) was added and the reaction mixture was stirred for 30 min or Meanwhile, the naphtalimide dye **42**[27a, 52] (250 mg, 0.7 mmol) dissolved in DCM (5 mL). It was added in one portion to the rea mixture, which was stirred on ice for additional 30 min. The ice bath removed and the reaction was stirred at RT for 72 hrs. The volatiles v evaporated. The residue was dissolved in EtOAc (50 mL) and was first with 0.5N HCl (30 mL x 3) and then with water (30 mL x 2). aqueous washings were extracted with EtOAc. The combined org fraction was washed again with 5% $NaHCO_3$ (30 mL x 3) and with w These washes were back extracted with EtOAc as well. Finally, combined organic layers were washed three times with brine and d over sodium sulfate. EtOAc was evaporated and the residue was pur on a silica gel column. The column was washed with two portion EtOAc:Hex (4:1), while the product was eluted later using $CHCl_3$:M (95:1). The final protected tripod was obtained as a bright yellow h viscous oil (398 mg, 75%). ^{1}H-NMR (400 MHz, $CDCl_3$): δ 0.96 (t, J= 3H), 1.40-1.45 (m, 6H), 1.70 (quint, *J* = 8.0 Hz, 2H), 2.39 (t, *J* = 5.7, 6H), 2.61-2.62 (m, 8H), 2.69 (t, *J* = 6.3, 2H), 3.18-3.23 (m, 13H), 3.48 (dd, *J*1= 11.3, J2=5.6 Hz, 6H), 3.66 (t, *J* = 5.7, 6H), 3.71 (s, 6H), 3.80 (bs, 2H), 3.88 (bs, 2H), 4.16 (t, *J* =8.0 Hz, 2H), 4.80 (s, 6H), 6.74 (s, 1H), 6.99 (bs, 3H), 7.19 (d, *J* = 8.0 Hz, 1H), 7.37 (m, 15H), 7.71 (t, *J* =8.0 Hz, 1H), 8.39 (d, *J* = 8.4 Hz, 1H), 8.50 (d, *J* =8.0 Hz, 1H), 8.58 (d, *J* =7.0 Hz, 1H). ^{13}C-NMR (400 MHz, $CDCl_3$): δ 13.89, 20.43, 27.99, 28.30, 31.42, 32.29,

33.42, 33.45, 34.64, 36.95, 40.16, 41.86, 45.48, 52.97, 59.96, 67.47, 69.29, 76.33, 115.38, 117.62, 123.45, 126.08, 126.28, 128.78, 129.34, 129.82, 131.21, 132.36, 134.20, 155.17, 163.94, 164.40, 170.69, 171.35, 172.69, 173.94. ESI-MS: calc.: 1326.65, found: 1327.00.

pH-dependent UV-Visible and Potentiometric Titrations. Proposed tripodal biomimetic analogs bind ferric ions starting from pH around 0 and the complexation is essentially complete much below pH of 2. Therefore, the stability constants of the first species formed in solution were determined from the spectrophotometric pH-dependent batch titrations carried out in pH range of around 0–2 (Plot S1a, Table S3), by following the changes in the intense LMCT band of the metal complex. These values were further used as constant values in spectrophotometric or potentiometric titrations carried out in pH range from 2 to 8 (Plot S1b, Table S3) to get the overall stability constants, logK_{FeL} (Table 1).

In the first series of experiments the stock solution of iron complexes was divided into various batches, with constant total volume of 2 mL, cFe = 0.0002 M and metal to ligand molar ratio 1:1. In pH range from 0.1 to 2, the pH was controlled by the concentration of the perchloric acid. Ionic strength was adjusted to 1 M with addition of $NaClO_4$. After preparation, each solution was allowed to equilibrate for 50-60 min, and then its visible spectrum was recorded using a Varian CARY 300 UV/Vis spectrophotometer.

In the second set of experiments, 15 mL of solution containing a 1:1 molar ratio of Fe^{III}:tripod with ferric concentration around 0.0002 M, were introduced into a jacketed cell ('Metrohm') maintained at 25.0±0.2 °C. The initial pH was adjusted to around 2 with $HClO_4$, and the titration of the complex (2 < pH < 11) was then carried out by addition of known volumes of 0.1 M sodium hydroxide by the Titrando 905 ('Metrohm') titrator. Simultaneous pH and UV-visible measurements (250 nm - 800 nm) were recorded using a Varian CARY 50 UV/Vis spectrophotometer fitted with C-Technologies optical fibers and immersion probe made of quartz ('C-Technologies') or metal ('Hellma' Ultra-Mini Immersion Probe). Both simultaneous with spectroscopic measurements and separate potentiometric titrations were performed using an automatic titrator system Titrando 905 ('Metrohm') with a combined glass electrode ('Mettler Toledo InLab Semi micro') with polymer filling (XEROLYT® EXTRA). The combined glass electrode was calibrated as a hydrogen concentration probe by titrating known amounts of $HClO_4$ (0.1 M) with CO_2-free NaOH solutions (0.1 M).[53] The cell was thermostated at 25.0 ± 0.2 °C. A stream of Argon, pre-saturated with water vapor, was passed over the surface of the solution. Before every experiment the exact concentration of ligand solution was determined by potentiometric titration of 3 mL of sample the ligand, with clig ~ 0.001 M. In separate potentiometric titrations metal to ligand ratio was 1:1 and the concentration of metal was 0.003 M. The ionic strength was fixed at I = 0.1 M with $NaClO_4$ ('Fluka', purum p.a.).

Analysis and Processing of the Data. The spectrophotometric data were analysed with Specfit program.[54] The potentiometric data (about 140 points collected over the pH range 2-11) were refined with the Superquad[55] or Hyperquad 2006[56] programs which use non-linear least-squares methods.[57] In the calculations of complex stability constants the protonation constants of free ligands and the hydrolysis constants related to $Fe(OH)^{2+}$ ($\log\beta_{11}$ = -2.56), $Fe(OH)^{2+}$ ($\log\beta_{12}$= -6.20), $Fe_2(OH)_2^{4+}$ ($\log\beta_{22}$= -2.84) and $Fe(OH)_3$ ($\log\beta_{13}$ = -11.41) species were taken into account.[58] In the calculation of complexes stability constants from spectrophotometric measurements, the fixed spectra of ferric ion in solution in pH 0.6 (for the first series of experiments) or 2.0 (for the second series of experiments) were included.[59]

Bacterial strains and growth media. *P. putida* JM218 strain and *U. maydis* sid$^-$ were provided by Y. Hadar. *E. coli* UT5600, ΔentC, ΔfhuA, ΔtonB, ΔfhuD, ΔfhuB and ΔfhuC[46] were purchased from The *E. coli* Genetic Stock Center at Yale. Bacteria were kept as glycerol stubs at -78ºC. Before each experiment bacteria were grown in standard LB medium overnight at 30ºC. MKB[60] medium was inoculated with the culture from LB and incubated for 24 hrs. To prepare iron depleted MKB for growth promotion experiments Purolite S910 resin (10g/L) was added to the medium. After stirring at RT for 5 hrs the resin was filtered off the medium was autoclaved. Trace iron(III) concentration levels confirmed by ICP-MS. *U. maydis* were grown under iron defi conditions as described previously.[49]

Bacterial growth measurement. Each growth promotion experi was conducted in triplicates. Bacteria were diluted in 30 mL of sterile depleted MKB medium to match the starting OD of 0.01 for *P. p* JM218 and of 0.02 for *E.coli* UT5600. Iron complexes of FC or the te analogs were added to the final concentration of $1.0\cdot10^{-6}$ M. Bacteria incubated at 30°C and their growth was monitored by measuring O 600 nm every 1-2 hrs until stationary phase.

Analog 1f uptake monitoring: Bacterial strains were taken fro glycerol stub (2–3 µL) and cultivated in sterile LB (3 mL with 0.1 mM concentration of kanamycin) for 10 hours at 30º C. Then, about 2–3 this bacterial stock were transferred into sterile MKB medium (3 mL 0.1mM final concentration of kanamycin) and grown under the s conditions for another 24 hours. Before introduction of our an bacterial samples (1 mL) were washed several times by addition of f MKB and centrifugation. FC uptake deletion mutants: ΔfhuA, Δt ΔfhuD, ΔfhuB and ΔfhuC produce enterobactin, which could scave iron from analog **1f**. They were washed thoroughly. After washings pellet was resuspended in fresh MKB (1 mL). Stock solutio fluorescent analog **1f** was dissolved in DDW to $4\cdot10^{-4}$ M, iron was ac in a 1:1 ratio from $FeCl_3$ stock solution ($1.73\cdot10^{-2}$ M; calibrated using MS) in HCl (1 N). This freshly prepared iron complex (10 µL) was ac to the bacterial sample at final concentration of $4\cdot10^{-6}$ M. For imaging bacterial cells (10 µL) were immobilized on a coverslip with 1% aga (30 µL). The coverslip was imaged on a DeltaVision microscope (' using EGFP and TL Brightfield channels at x100. Epi-fluores excitation was performed using a DAPI filter at 488 nm and emission recorded using a GFP filter at 509 nm. All images were acquired u identical conditions. Images were subsequently analyzed using ZE software.

Funding Sources

We are grateful to the Polish National Science Center (N[illegible], UMO-2011/03/B/ST5/01057) for financial support.

We would like to express our gratitude to the Gerhardt M. J. Schmidt Minnerva Center on Supermolecular Architecture, the Helen and Martin Kimmel Center for Molecular Design and the

Kimmelman Center for Macromolecular Assemblies for financial support.

Acknowledgements

We thank Prof. U. Banin and his team, from the Institute of Chemistry, The Hebrew University of Jerusalem for kindly supplying us with carboxylate functionalized QDs.

Keywords: Biomimetic chemistry • Siderophores • Ferrichrome• Fluorescent conjugates • Quantum Dots

[1] a) J. B. Neilands, *Annu. Rev. Nutr.* **1981**, *1*, 27-46; b) C. Wandersman, P. Delepelaire, *Annual Review of Microbiology* **2004**, *58*, 611-647; c) M. L. Guerinot, *Annual Review of Microbiology* **1994**, *48*, 743-772.

[2] a) M. Miethke, M. A. Marahiel, *Microbiol. Mol. Biol. Rev.* **2007**, *71*, 413-451; b) D. E. Crowley, Y. C. Wang, C. P. P. Reid, P. J. Szaniszlo, *Plant Soil* **1991**, *130*, 179-198; c) B. C. Chu, A. Garcia-Herrero, T. H. Johanson, K. D. Krewulak, C. K. Lau, R. S. Peacock, Z. Slavinskaya, H. J. Vogel, *Biometals* **2010**, *23*, 601-611; d) F. Pattus, M. A. Abdallah, *J. Chin. Chem. Soc.* **2000**, *47*, 1-20.

[3] M. Hannauer, Y. Barda, G. L. A. Mislin, A. Shanzer, I. J. Schalk, *J Bacteriol* **2010**, *192*, 1212-1220.

[4] a) D. J. Raines, T. J. Sanderson, A. K. Duhme-Klair, E. Wilde, in *Elsevier Reference Module in Chemistry, Molecular Sciences and Chemical Engineering*, Elsevier, **2015**; b) R. Chakraborty, in *Iron Uptake in Bacteria with Emphasis on E. coli and Pseudomonas* (Eds.: R. Chakraborty, V. Braun, K. Hantke, P. Cornelis), Springer Netherlands, Dordrecht, **2013**, pp. 1-29; c) V. Braun, *Front Biosci* **2003**, *8*, 1409-1421; d) D. van der Helm, R. Chakraborty, in *Microbial Transport Systems*, Wiley-VCH Verlag GmbH & Co. KGaA, **2003**, pp. 261-287.

[5] I. J. Schalk, L. Guillon, *Amino Acids* **2013**, *44*, 1267-1277.

[6] H. Boukhalfa, A. L. Crumbliss, *Biometals* **2002**, *15*, 325-339.

[7] R. Codd, *Coord. Chem. Rev.* **2008**, *252*, 1387-1408.

[8] a) J. B. Neilands, *J. Am. Chem. Soc.* **1952**, *74*, 4846-4847; b) J. B. Neilands, *Science* **1967**, *156*, 1443-1447; c) S. J. Rogers, R. A. Warren, J. B. Neilands, *Nature* **1963**, *200*, 167.

[9] M. Gaspar, M. A. Santos, K. Krauter, G. Winkelmann, *Biometals* **1999**, *12*, 209-218.

[10] a) A. Shanzer, J. Libman, *J. Chem. Soc., Chem. Commun.* **1983**, 846-847; b) E. J. Corey, S. Bhattacharyya, *Tetrahedron Letters* **1977**, 3919-3922; c) J. M. Roosenberg, Y. M. Lin, Y. Lu, M. J. Miller, *Curr. Med. Chem.* **2000**, *7*, 159-197; d) R. Mashiach, M. M. Meijler, *Org. Lett.* **2013**, *15*, 1702-1705; e) M. Meyer, J. R. Telford, S. M. Cohen, D. J. White, J. Xu, K. N. Raymond, *J. Am. Chem. Soc.* **1997**, *119*, 10093-10103; f) J. Hu, M. J. Miller, *J. Am. Chem. Soc.* **1997**, *119*, 3462-3468; g) J. Deng, Y. Hamada, T. Shioiri, *J. Am. Chem. Soc.* **1995**, *117*, 7824-7825; h) P. J. Maurer, M. J. Miller, *J. Am. Chem. Soc.* **1982**, *104*, 3096-3101; i) J. L. H. Madsen, T. C. Johnstone, E. M. Nolan, *J. Am. Chem. Soc.* **2015**, *137*, 9117-9127; j) D. Seebach, H.-M. Müller, H. M. Bürger, D. A. Plattner, *Ache, Angew. Chem. Int. Ed. Engl* **1992**, *31*, 434-435; k) R. J. Bergeron, J. J. Pegram, *J. Org. Chem.* **1988**, *53*, 3131-3134.

[11] A. Ino, A. Murabayashi, *Tetrahedron* **2001**, *57*, 1897-1902.

[12] T. Zheng, J. L. Bullock, E. M. Nolan, *J. Am. Chem. Soc.* **2012**, *134*, 18388-18400.

[13] R. Breslow, *Chem. Soc. Rev* **1972**, *1*, 553-580.

[14] a) T. Lifa, W. Tieu, R. K. Hocking, R. Codd, *Inorg. Chem.* **2015**, *54*, 3573-3583; b) S. Heggemann, U. Mollmann, P. Gebhardt, L. Heinisch, *Biometals* **2003**, *16*, 539-551; c) S. K. Sharma, M. J. Miller, S. M. Payne, *J. Med.Chem.* **1989**, *32*, 357-367; d) S. Dhungana, J. M. Harrington, P. Geblhardt, U. Mollmann, A. L. Crumbliss, *Inorg. Chem.* **2007**, *46*, 8362-8371; e) B. H. Lee, M. J. Miller, C. A. Prody, J. B. Neilands, *J. Med. Chem.* **1985**, *28*, 317-323; f) B. H. Lee, M. J. Miller, C. A. Prody, J. B. Neilands, *J. Med. Chem.* **1985**, *28*, 323-327; g) K. Matsumoto, T. Ozawa, K. Jitsukawa, H. Masuda, *Inorg. Chem.* **2004**, *43*, 8538-8546.

[15] a) A. Shanzer, J. Libman, R. Lazar, Y. Tor, *Pure Appl. Chem.* **1989**, *61*, 1529-1534; b) A. Shanzer, J. Libman, R. Lazar, Y. Tor, T. Emery, *Biochem. Bioph. Res. Co.* **1988**, *157*, 389-394; c) E. Jurkevitch, Y. Hadar, Y. Chen, J. Libman, A. Shanzer, *J Bacteriol* **1992**, *174*, 78-

[16] a) T. Emery, L. Emery, R. K. Olsen, *Biochem. Bioph. Res. Co.* **1** *119*, 1191-1197; b) R. K. Olsen, K. Ramasamy, *J. Org. Chem.* **198** 2264-2271.

[17] A. Shanzer, J. Libman, P. Yakirevitch, Y. Hadar, Y. Chen, E. Jurke *Chirality* **1993**, *5*, 359-365.

[18] E. Jurkevitch, Y. Hadar, Y. Chen, J. Libman, A. Shanzer, *J. Bact* **1992**, *174*, 78-83.

[19] a) H. Weizman, O. Ardon, B. Mester, J. Libman, O. Dwir, Y. Hada Chen, A. Shanzer, *J. Am. Chem. Soc.* **1996**, *118*, 12368-12375; Nudelman, O. Ardon, Y. Hadar, Y. N. Chen, J. Libman, A. Shanz *Med. Chem.* **1998**, *41*, 1671-1678.

[20] L. Zelikovich, J. Libman, A. Shanzer, *Nature* **1995**, *374*, 790-792.

[21] I. Rubinstein, S. Steinberg, Y. Tor, A. Shanzer, J. Sagiv, *Nature* **1** *332*, 426-429.

[22] a) A. D. Ferguson, E. Hofmann, J. W. Coulton, K. Diederichs, W. W *Science* **1998**, *282*, 2215-2220; b) K. P. Locher, B. Rees, R. Koe A. Mitschler, L. Moulinier, J. P. Rosenbusch, D. Moras, *Cell* **1998** 771-778.

[23] K. D. Krewulak, H. J. Vogel, *Biochim. Biophys. Acta* **2008**, *1778*, 1 1804.

[24] E. Olshvang, A. Szebesczyk, H. Kozlowski, Y. Hadar, E. Gumie Kontecka, A. Shanzer, *Dalton Trans.* **2015**, *44*, 20850-20858.

[25] W. R. Harris, C. J. Carrano, K. N. Raymond, *J. Am. Chem. Soc.* **1** *101*, 2722-2727.

[26] a) B. H. Lee, M. J. Miller, *J. Org. Chem.* **1983**, *48*, 24-31; b) R. Grig Rankovic, M. Thoroughgood, *Tetrahedron* **2000**, *56*, 8025-8032.

[27] a) M. M. Meijler, R. Arad-Yellin, Z. I. Cabantchik, A. Shanzer, *J. Chem. Soc.* **2002**, *124*, 12666-12667; b) R. Nudelman, O. Ardo Hadar, Y. Chen, J. Libman, A. Shanzer, *J. Med. Chem.* **1998**, *41*, 1 1678.

[28] J. B. Neilands, *J. Biol. Chem.* **1995**, *270*, 26723-26726.

[29] L. D. Pettit, H. K. Powell, Timble, York, UK, **2001**, (www.acadsoft.c version 5.6).

[30] G. Anderegg, F. L'Eplattenier, G. Schwarzenbach, *Helv. Chim.* **1963**, *46*, 1409-1422.

[31] W. R. Harris, C. J. Carrano, S. R. Cooper, S. R. Sofen, A. E. Avde V. Mcardle, K. N. Raymond, *J. Am. Chem. Soc.* **1979**, *101*, 6097-6

[32] a) A. M.,Albrecht-Gary, A.L. Crumbliss, *Vol. 35* (Ed.: A. Sigel, H. S Marcel Dekker, New York, **1998**, p. 239; b) A. L. Crumbliss, *Hand of Microbial Iron Chelates*, (Ed.: G. Winkelmann). CRC Press: Raton, Florida, **1991,** pp. 177.

[33] a) E. Farkas, P. Buglyo, *J. Chem. Soc., Dalton Trans.* **1990**, 1549-1551; b) E. Farkas, D. A. Brown, R. Cittaro, W. K. Glass, *J. Chem. Soc., Dalton Trans.* **1993**, 2803-2807.

[34] M. E. Elish, J. R. Pierce, C. F. Earhart, *J. Gen. Microbiol.* **1988**, *134*, 1355-1364.

[35] B. Schwyn, J. B. Neilands, *Anal. Biochem.* **1987**, *160*, 47-56.

[36] R. C. Hider, X. Kong, *Nat. Prod. Rep.* **2010**, *27*, 637-657.
[37] I. J. Schalk, G. L. A. Mislin, K. Brillet, *Curr. Top. Membr .***2012**, *69*, 37-66.
[38] a) G. Winkelmann, V. Braun, *Fems Microbiol. Lett.* **1981**, *11*, 237-241; b) H. U. Naegeli, W. Kellerschierlein, *Helv. Chim. Acta* **1978**, *61*, 2088-2095.
[39] S. Dhungana, P. S. White, A. L. Crumbliss, *J. Biol. Inorg. Chem.* **2001**, *6*, 810-818.
[40] H. Schwarz, A. L. Koch, *Microbiology* **1995**, *141*, 3161-3170.
[41] E. K. Dolence, A. A. Minnick, M. J. Miller, *J. Med. Chem.* **1990**, *33*, 461-464.
[42] V. Braun, K. Hantke, in *Microbial transport systems* (Ed.: G. Winkelmann), Wiley-VCH, Weinheim, **2002**, pp. 289-312.
[43] R. Chakraborty, E. Storey, D. van der Helm, *Biometals* **2007**, *20*, 263-274.
[44] a) K. Postle, R. A. Larsen, *Biometals* **2007**, *20*, 453-465; b) M. C. Wiener, *Curr Opin Struct Biol* **2005**, *15*, 394-400.
[45] K. N. Raymond, B. E. Allred, A. K. Sia, *Acc. Chem. Res.* **2015**, *48*, 2496-2505.
[46] T. Baba, T. Ara, M. Hasegawa, Y. Takai, Y. Okumura, M. Baba, K. A. Datsenko, M. Tomita, B. L. Wanner, H. Mori, *Mol. Syst. Biol.* **2006**, 1-11.
[47] B. Winterberg, S. Uhlmann, U. Linne, F. Lessing, M. A. Marahiel, H. Eichhorn, R. Kahmann, J. Schirawski, *Mol. Microbiol.* **2010**, *75*, 1260-1271.
[48] M. W. Lewis, I. V. Robalino, N. O. Keyhani, *Microbiology* **2009**, *155*, 3110-3120.
[49] O. Ardon, R. Nudelman, C. Caris, J. Libman, A. Shanzer, Y. Chen, Y. Hadar, *J. Bacteriol.* **1998**, *180*, 2021-2026.
[50] a) D. D. Doorneweerd, W. A. Henne, R. G. Reifenberger, P. S. Low, *Langmuir* **2010**, *26*, 15424-15429; b) T. Inomata, T. Murase, H. Ido, T. Ozawa, H. Masuda, *Chem. Lett.* **2014**, *43*, 1146-1148; c) T. Inomata, H. Eguchi, Y. Funahashi, T. Ozawa, H. Masuda, *Langmuir* **2012**, *28*, 1611-1617; d) T. Inomata, H. Eguchi, K. Matsumoto, Y. Funahashi, T. Ozawa, H. Masuda, *Biosens. Bioelectron.* **2007**, *23*, 751-755; e) Y. Kim, D. P. Lyvers, A. Wei, R. G. Reifenberger, P. S. Low, *Lab Chip* **2012**, *12*, 971-976; f) T. Zheng, E. M. Nolan, *Metallomics* **2012**, *4*, 866-880.
[51] a) S. Ruhle, M. Shalom, A. Zaban, *Chemphyschem* **2010**, *11*, 2290-2304; b) H. Tsukigase, Y. Suzuki, M. H. Berger, T. Sagawa, S. Yoshikawa, *J. Nanosci. Nanotechnol.* **2011**, *11*, 1914-1922.
[52] C. Y. Li, X. B. Zhang, L. Qiao, Y. Zhao, C. M. He, S. Y. Huan, L. M. Lu, L. X. Jian, G. L. Shen, R. Q. Yu, *Anal. Chem.* **2009**, *81*, 9993-10001.
[53] P. Gans, B. O'Sullivan, *Talanta* **2000**, *51*, 33-37.
[54] a) H. Gampp, M. Maeder, C. J. Meyer, A. D. Zuberbuehler, *Talanta* **1986**, *33*, 943-951; b) H. Gampp, M. Maeder, C. J. Meyer, A. D. Zuberbuhler, *Talanta* **1985**, *32*, 95-101; c) H. Gampp, M. Maeder, C. J. Meyer, A. D. Zuberbuhler, *Talanta* **1985**, *32*, 257-264; d) F. J. Rossotti, H. S. Rossotti, R. J. Whewell, *J. Inorg. Nucl. Chem.* **1971**, *33*, 2051-2065.
[55] P. Gans, A. Sabatini, A. Vacca, *J. Chem. Soc. Dalton* **1985**, 1195-1200.
[56] P. Gans, A. Sabatini, A. Vacca, *Talanta* **1996**, *43*, 1739-1753.
[57] P. Gans, *Data Fitting in the Chemical Sciences: By the Method of Least Squares*, Wiley, Chichester, **1992**.
[58] C. F. Baes, R. E. Mesmer, *The hydrolysis of cations*, Wiley, New York, **1976**, pp. 489
[59] a) R. M. Milburn, W. C. Vosburgh, *J. Am. Chem. Soc.* **1955**, *77*, 1352-1355; b) R. M. Milburn, *J. Am. Chem. Soc.* **1957**, *79*, 537-540.
[60] M. Höfte, K. Y. Seong, E. Jurkevitch, W. Verstraete, in *Iron Nutrition and Interactions in Plants: "Proceedings of the Fifth International Symposium on Iron Nutrition and Interactions in Plants", Jerusalem, Israel, 1989* (Eds.: Y. Chen, Y. Hadar), Springer Netherlands, Dordrecht, **1991**, pp. 289-297.

10.1002/chem.201702647

WILEY-VCH

FULL PAPER

A 'true' analog matching Ferrichrome (FC) in cross-phylum activity, uptake pathway and iron affinity is described. This fluorescently labeled analog sheds light on the fate of siderophores following iron delivery and provides a tool for identifying microbial targets. Quantum Dots (QD) decorated with this analog trigger cluster formation by FC-recognizing bacteria, suggesting a method for microbial concentration and separation.

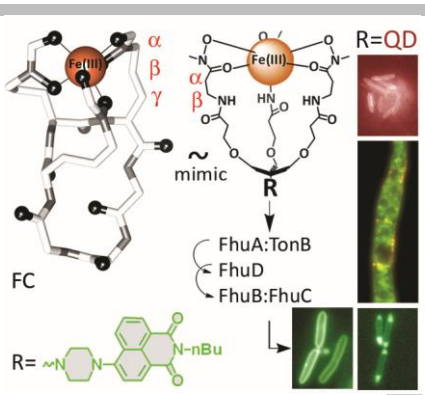

Jenny Besserglick, Evgenia Olshvang, Agnieszka Szebesczyk, Joseph Englander, Dana Levinson, Yitzhak Hadar, Elzbieta Gumienna-Kontecka, and Abraham Shanzer**

Page No. – Page No.

Ferrichrome has found its match: biomimetic analogs with diversified activity map discrete microbial targets

10.1002/chem.201702647